Journal of Hazardous Materials 170 (2009) 449–456

Contents lists available at ScienceDirect

Journal of Hazardous Materials

journal homepage: www.elsevier.com/locate/jhazmat

Effect of particle spatial distribution on particle deposition in ventilation rooms

Bin Zhao*, Jun Wu

Dept. of Building Science, School of Architecture, Tsinghua University, Beijing, China

ARTICLE INFO

Article history:
Received 13 January 2009
Received in revised form 20 April 2009
Accepted 20 April 2009
Available online 24 April 2009

Keywords:
Ventilation
Indoor air quality (IAQ)
Aerosol
Particle
Deposition

ABSTRACT

We used simulations and experimental tests to investigate indoor particle deposition during four commonly used ventilation modes, including ceiling supply, side-up supply, side-down supply and bottom supply. We used a condensation monodisperse aerosol generator to generate fine diethylhexyl sebacate (DEHS) particles of different sizes along with two optical particle counters that measured particle concentration at the exhaust opening and inside a three-dimensional ventilated test room. We then simulated particle deposition using the same ventilation modes with computational fluid dynamics (CFD) method. Our simulated results indicate that mean deposition velocity/rate for particles 0.5–10 μm (aerodynamic diameter) is not affected by different ventilation modes. However, both our experimental and simulated results indicate that the deposition loss factor, a parameter defined based on mass balance principle to reflect the influence of particle distribution on deposited particle quantity, differ significantly by ventilation mode. This indicates that ventilation plays an important role in determining particle deposition due to the apparent differences in the spatial distribution of particles. The particle loss factor during ventilation modes characterized by upward air flow in the room is smaller than that of mixing ventilation; however this trend was strongly influenced by the relative location of the inlets, outlets and aerosol source.

1. Introduction

Deposition of aerosol particles indoors has received increasing attention due to the growing concern about the human health effects of particle pollution exposure. The deposition process appears to effect human exposure to particle pollution by altering the size distribution of indoor particles. At the same time, particle deposition may lead to material degradation in households and other buildings, including damage to artwork or electronic equipment. Thus, it is important to understand the determinants of particle deposition quantity for evaluating indoor air quality (IAQ) and informing the design and evaluation of ventilation systems.

A number of studies discuss indoor particle deposition and several compare particle deposition in different indoor environments. Experimental methods [1–13] and lumped parameter models [1,14–18] introduced the use of mean deposition velocity and deposition rate for estimating the deposition quantity of particles. Further, numerical simulation studies using computational fluid dynamics (CFD) examined indoor particle deposition by either tracking particle trajectories using the Lagrangian formulation [19–21] or by calculating the particle deposition rate to wall surfaces using the Eulerian framework [22,23]. To our knowledge, however, just two studies have analyzed the effect of different ventilation modes on particle deposition. Past studies have typically not accounted for differences in the quantity of deposited particles using different ventilation modes with a constant ventilation rate, particle size and density, and generating source. Under real-life conditions, the quantity of deposited particles may greatly vary under different ventilation flow patterns even in cases when the deposition rate or average deposition velocity is held constant by a stable ventilation rate. This hypothesis has been tested and validated in several previous investigations [21,22,24,25]. As ventilation is a commonly applied strategy for reducing air pollution in the indoor environment, it is important to understand how use of different ventilation modes may influence particle deposition indoors.

A 2005 study used both numerical simulations and actual measurements to determine particle decay rates during three different ventilation modes using the Lagrangian formulation [24]. However, the ventilation rates used in this study (0.5 and 1.0 air change per hour (ACH)) are substantially lower than what is typically observed in a room that combines ventilation with air cooling or heating (5.0–8.0 ACH). A more recent study simulated particle deposition using two commonly observed ventilation modes (i.e., mixing and displacement ventilation) [25]. However, the limited number of ventilation modes tested in this study does not adequately represent the range of modes being installed into new buildings. Further,

* Corresponding author. Tel.: +86 10 62779995; fax: +86 10 62773461.
E-mail address: binzhao@tsinghua.edu.cn (B. Zhao).

0304-3894/$ – see front matter © 2009 Elsevier B.V. All rights reserved.
doi:10.1016/j.jhazmat.2009.04.079

these simulated results have not yet been validated by experimental tests.

We evaluated indoor particle deposition using both experimental tests and numerical simulation. We used four different ventilation modes representing the most commonly used ventilation modes in modern buildings to test the effect of spatial distribution of particles on particle deposition quantity.

2. Methods and materials

2.1. Experimental tests

We measured particle deposition and concentration in a 30 m^3 test room (Length(X) × Height(Y) × Width(Z) = 4 m × 2.5 m × 3 m) equipped with a mechanical ventilation system that can replicate various indoor environmental conditions. The air supply flow rate of the test room was held at a constant 8.0 ACH using an electronic fan speed control and nozzle flowmeter as illustrated in Fig. 1(a). The room was under positive pressure during each test. We sealed the testing room by positioning a rubber strip along the entrance door's edges in order to prevent sample concentration from ambient air particles. Additionally, we installed a high-efficiency particle filter (HEPA) and alternated use of the air supply and exhaust system to eliminate use of recycled air and, subsequently, decrease the potential for supply air contamination.

The four ventilation modes used in this study are described in Table 1, specifically ceiling supply, side-up supply, side-down supply and bottom supply. We tested these modes by alternating air supply openings and exhaust outlet accordingly. The configuration of the four ventilation modes is illustrated in Fig. 1(b). All of the inlets and outlets were symmetrical with the test room's center plane (Z = 1.5 m). The four cases are isothermal cases, i.e., there is no temperature difference between supply air and indoor air, and there are no heat sources as well. The walls of the test chamber are adiabatic. The supply air velocity for each case is measured by dividing the air supply opening into sub-rectangles, and the measured value is employed as boundary conditions for numerical simulation (shown in Table 2).

We used a condensation monodisperse aerosol generator (Model 3475; TSI Inc., St. Paul, MN) to generate fine diethylhexyl sebacate (DEHS) particles. The density of generated particles (914 kg/m^3) is approximately equal to the density of water; thus, the particle diameter is approximately equal to its aerodynamic diameter. The particle source strength is stable and the geometric standard deviation is less than 1.10 from 0.5 to 8 μm and less than 1.25 from 0.1 to 0.5 μm, according to the instruction manual of the aerosol generator [26]. Also according to the instruction manual of the aerosol generator [26], different sized particles could be produced by adjusting some parameters when generating. Increasing either the saturator temperature or the flow rate of the saturator or screen could result in an increase in the particle size produced by the generator. According to the equations and

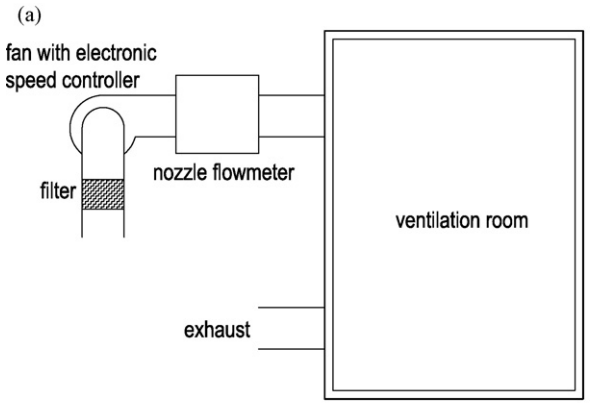

Schematic of the mechanical ventilation system and test room

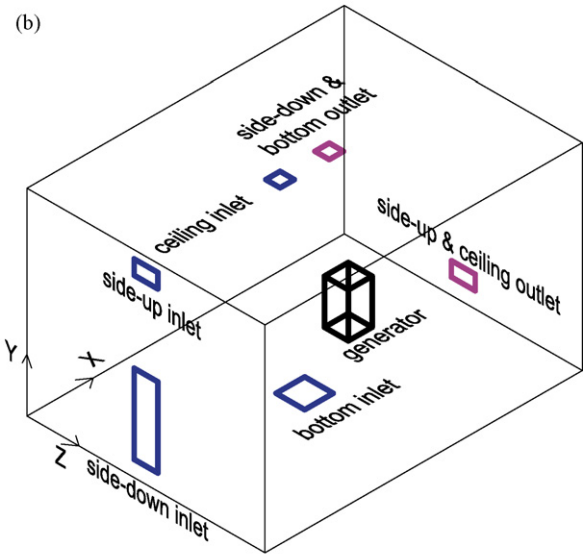

Schematic of the test room and its various inlets and outlets

Fig. 1. Schematic of the experimental design.

the figures provided in the instruction manual, three sizes of fine and course particles (0.75, 1.5 and 10 μm) are generated. In particular, 10 μm-sized particles could be generated by using the same parameters in the Figure A-3 in the instruction with the saturator temperature changing from 220 to 240 °C [26]. The particle generator (Length(X) × Height(Y) × Width(Z) = 0.3 m × 0.56 m × 0.3 m) was symmetrically positioned along the test room's center plane, as shown in Fig. 1(b).

We used two optical particle counters (FLUKE 983, FLUKE Inc.) to measure indoor particle concentration. The Fluke 983 simultane-

Table 1
Configuration of the four ventilation modes.

Ventilation modes	Inlet							Outlet						
	Xs[a]	Xe[a]	Ys[b]	Ye[b]	Zs[c]	Ze[c]	Type	Xs[a]	Xe[a]	Ys[b]	Ye[b]	Zs[c]	Ze[c]	Type
Ceiling supply	1.6	1.78	2.5	2.5	1.41	1.59	Diffuser	4	4	0.2	0.38	1.35	1.65	Grille
Side-up supply	0	0	2.22	2.4	1.41	1.59	Register	4	4	0.2	0.38	1.35	1.65	Grille
Side-down supply	0	0	0.2	1.2	1.35	1.65	Perforated panel	2.22	2.4	2.5	2.5	1.41	1.59	Grille
Bottom supply	1.82	2.18	0	0	1.32	1.68	Perforated panel	2.22	2.4	2.5	2.5	1.41	1.59	Grille

[a] Xs and Xe denote the start and end location in X axis;
[b] Ys and Ye denote the start and end location in Y axis;
[c] Zs and Ze denote the similar meaning in Z axis.

Table 2
Inlet velocity distribution.

Ventilation modes	Inlet velocity distribution			
	Sketch map	Velocity direction	Velocity (m/s)	
Ceiling supply	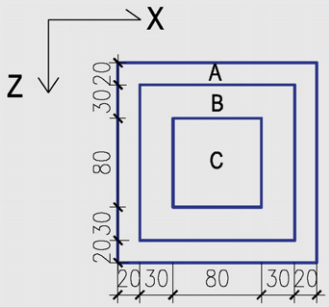	 Downward and away from the center of the inlet at a 45-degree angle	Section A Section B Section C	6.523 0.817 0
Side-up supply	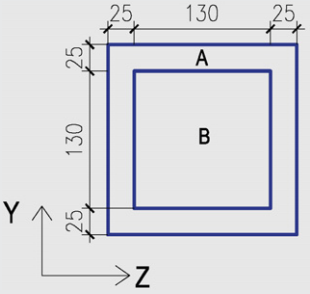	 Perpendicular to the inlet	Section A Section B	3.48 0.506
Side-down supply	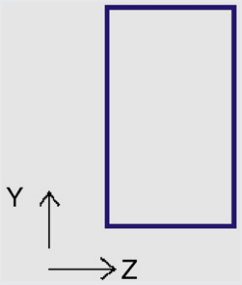	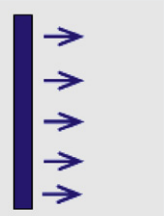 Perpendicular to the inlet	All the inlet	0.222
Bottom supply	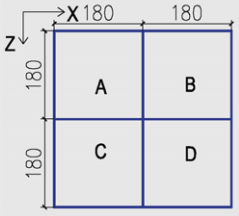	 Perpendicular to the inlet	Section A and section D Section B and section C	0.572 0.456

ously measures and records six channels of particle size distribution (0.3, 0.5, 1.0, 2.0, 5.0 and 10.0 μm). The counter has a coincidence loss of 5% when the particle concentration is 2,000,000 particles per cubic inch and a 100% counting efficiency when the measured particle diameter is larger than 0.45 μm [27]. We calibrated the counter using a Zero Counter Filter prior to each measurement. It should be noted that since the TSI 3475 aerosol generator produces just three particle sizes (0.75, 1.5 and 10 μm), the measurements recorded by the optical particle counter's 0.5, 1.0, 5 and 10.0 μm channel (i.e., the 0.5–1 μm, 1–2 μm, 5.0–10.0 μm and >10.0 μm diameter range) will be identical to the measured concentration of 0.75, 1.5 and 10 μm particles produced by the aerosol generator respectively [27].

Approximately 20 min after activating the ventilation system at a predetermined airflow rate (8.0 ACH), we began continuously generated particles at a constant volume using the TSI aerosol generator . We divided the exhaust outlet of the ventilation room into 4 rectangles and measured the particle concentration at the center of each rectangle until particle concentration in the room reached a steady state. Prior to changing the ventilation point in the test room, a trained technician entered the test room, moved the OPC devices to a different ventilation point and then exited the test room to conduct the next measurement. To avoid particle resuspension, we waited approximately 15 min after the technician had exited the room to resume measurements under the assumption that the particle concentration in the test room had returned to a constant level.

We used the particle mass/count balance principle to determine particle deposition:

$$S_{\text{deposition}} = S_{\text{generator}} - C_{\text{outlet}} \cdot Q, \quad (1)$$

where Q is supply air flow rate (m^3/s), which was equal to 240 m^3/h (0.067 m^3/s, equally the air change rate is 8.0 ACH) in both the experiments and simulations. We measured the particle concentration at the exhaust outlet, C_{outlet} (particles/m^3) (equal to the

Table 3
The simulated mean deposition velocity ($V_{d,total}$) and deposition rate (k) using four ventilation modes.

		Ceiling	Bottom	Side-up	Side-down
d_p = 0.75 μm	$V_{d,total}$ (m/s)	4.21E−06	4.10E−06	4.31E−06	4.09E−06
	$\frac{V_{d,floor} \cdot A_{floor}}{A_{total}}$ (m/s)	4.01E−06	4.01E−06	4.01E−06	4.01E−06
	k (s^{-1})	8.28E−06	8.06E−06	8.48E−06	8.04E−06
d_p = 1.5 μm	$V_{d,total}$ (m/s)	1.47E−05	1.46E−05	1.48E−05	1.46E−05
	$\frac{V_{d,floor} \cdot A_{floor}}{A_{total}}$ (m/s)	1.46E−05	1.46E−05	1.46E−05	1.46E−05
	k (s^{-1})	2.89E−05	2.87E−05	2.91E−05	2.87E−05
d_p = 10 μm	$V_{d,total}$ (m/s)	5.93E−04	5.93E−04	5.93E−04	5.93E−04
	$\frac{V_{d,floor} \cdot A_{floor}}{A_{total}}$ (m/s)	5.93E−04	5.93E−04	5.93E−04	5.93E−04
	k (s^{-1})	1.17E−03	1.17E−03	1.17E−03	1.17E−03

average value of the 4 measured points at the outlet), while the supply particle concentration was nearly zero and the particle generating rate, $S_{generator}$ (particles/s), was known, it is easy to get the particle deposition quantity, $S_{deposition}$ (particles/s) by Eq. (1).

As the particle generation rate, $S_{generator}$, was not included in the aerosol generator instruction manual, we conducted an additional experiment to determine this value for the test room. Holding the air change rate at 8 ACH, we placed the aerosol generator near the exhaust outlet (the side-down inlet and the side-up and ceiling outlet were employed) to test the particle generation rate. The near piston flow outflow of air by the exhaust outlet largely prevented particles from depositing in the room. Thus, we estimated the particle generation rate, $S_{generator}$, by multiplying the particle concentration at the exhaust outlet (C_{out}) by the supply air flow rate (Q).

2.2. Simulation tests

To calculate the three-dimensional turbulent airflow in ventilated rooms efficiently and with increased precision, we applied a well-validated and simplified methodology that combines an N-point air supply opening model [28] with a zero equation turbulence model [29]. We used a drift flux model to simulate the indoor aerosol particles distribution. This particular model uses an Eulerian approach that integrates the gravitational settling effects of particles into the particle concentration transportation equation. This model builds on the traditional transportation model for gas contaminants by adding the drift flux term into the particle concentration equation, which is caused by the particles' slip velocity and the drag force of air. The particle deposition boundary conditions for walls are based on the analytical expression of deposition velocity developed by Lai and Nazaroff [30]. The friction velocity of walls is the key input parameter for quantifying particle deposition velocity and related particle flux to the wall, which can be calculated using the data on wall shear stress. We combined the drift flux model combined with the particle deposition boundary conditions of wall surfaces using STACH-3, a three-dimensional CFD program developed by Zhao et al. [28], the details of which can be found in [22].

The grid numbers calculated for ceiling supply mode are $47(X) \times 30(Y) \times 39(Z)$, $45(X) \times 33(Y) \times 38(Z)$ for bottom supply mode, $43(X) \times 35(Y) \times 37(Z)$ for side-up supply mode, and $38(X) \times 26(Y) \times 37(Z)$ for side-down supply mode, respectively. We conducted a grid independence test by calculating the same mode with finer grids (twice denser in each direction) and found little changes in our results. The air flow into the optical particle counter was not included in the CFD simulation as it is generally considered negligible.

3. Analysis and results

To understand the effect of ventilation modes on particle deposition, an important consideration is how to measure indoor particles with precision. It is therefore important to validate the methods employed for simulation. The numerical model has been validated in previous studies [25,31], all of which indicated that there was sufficient agreement between the simulations and actual measurements.

3.1. Particle deposition velocity and deposition rate

The area-weighted deposition velocity (also known as mean deposition velocity), $V_{d,total}$, is defined as:

$$V_{d,total} = \frac{V_{d,wall} \cdot A_{wall} + V_{d,ceiling} \cdot A_{ceiling} + V_{d,floor} \cdot A_{floor}}{A_{total}}, \quad (2)$$

where A_{wall}, $A_{ceiling}$ and A_{floor} is the area of the vertical walls, ceiling and floor, respectively (m^2); A_{total} is the total surface wall area (i.e., the sum of A_{wall}, $A_{ceiling}$ and A_{floor}) (m^2); and finally, $V_{d,wall}$, $V_{d,ceiling}$ and $V_{d,floor}$ are the deposition velocities of particles onto the vertical walls, ceiling and floor, respectively (m/s).

And the deposition rate, k (s^{-1}), is calculated by:

$$k = \frac{V_{d,total} A_{total}}{V}, \quad (3)$$

where V is the volume of the ventilation room in cubic meters.

As mean deposition velocity is difficult to quantify using experimental tests, we used numerical calculated results for analysis as previous studies suggest that they agree with actual measured values [25,31]. We estimated air friction velocity using the CFD method and particle deposition velocity using the analytical three-layer Eulerian model by Lai and Nazaroff [30]. The estimated mean deposition velocity and deposition rate of the four ventilation modes are displayed in Table 3.

As shown in Table 3, both mean particle deposition velocity and particle deposition rate are not affected by changes in ventilation mode when the particle size falls into the 0.75–10 μm range (aerodynamic diameter). The reason is gravitational settling play the most important role in particle deposition in these cases. Also as shown in Table 3 $(V_{d,floor} \cdot A_{floor})/A_{total}$ was almost equal to the mean particle deposition velocity which implies the deposition velocity to the floor, $V_{d,floor}$, is considerably faster than to other room surfaces. For this reason, friction velocity should not influence the deposition velocity. This is supported by our results shown in Fig. 2. The friction velocity for all the ventilation strategies was within the 0.6–6.0 cm/s range according to the numerical calculation.

Our finding that average deposition velocity/rate is not affected by different ventilation modes suggests that use of traditional parameters would provide the same particle deposition quantity

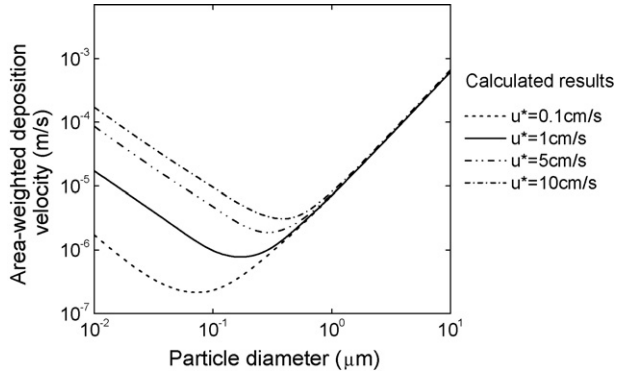

Fig. 2. Calculated area-weighted deposition velocity.

Table 4
The measured and simulated particle deposition loss factor.

Ventilation mode		Ceiling	Bottom	Side-up	Side-down
$L(d_p = 0.75\ \mu m)$	Measured	4.88%	–	–	1.59%
	Simulated	0.09%	0.27%	0.36%	0.23%
$L(d_p = 1.5\ \mu m)$	Measured	–	4.30%	6.51%	0.99%
	Simulated	0.30%	0.95%	1.21%	0.82%
$L(d_p = 10\ \mu m)$	Measured	13.52%	23.08%	27.44%	24.87%
	Simulated	9.62%	22.45%	32.47%	22.10%

as if the particle generating sources ($S_{generator}$) and ventilation rate (Q) were the same. This can be deduced from the widely used mathematical model of indoor particle dynamics:

$$S_{deposition} = \frac{k \cdot V \cdot S_{generator}}{Q + k \cdot V} \quad (4)$$

Despite the minimal difference in mean deposition velocity/rate between the ventilation modes, the deposited particle quantity could significantly differ due to the considerable difference in particle spatial distribution discussed in the following section.

3.2. Deposition loss factor

To incorporate the effect of particle distribution on particle deposited quantity, we defined the particle penetrating factor P and particle deposition loss factor L as follows:

$$P = \frac{Q \cdot C_{outlet}}{S_{generator}}$$
$$L = 1 - P \quad (5)$$

Based on the mass balance principle, the particle deposition loss factor L could also be calculated as follows:

$$L = \frac{S_{generator} - Q \cdot C_{outlet}}{S_{generator}} = \frac{S_{deposition}}{S_{generator}}, \quad (6)$$

where L represents the deposited particle quantity for different ventilation modes.

It should be noted that the traditional particle deposition rate assumes that particle concentration is uniform under well-mixed condition and can only be evaluated from the deposition velocity and enclosure geometry. Particle loss factor accounts for the

Table 5
The non-dimensional mean concentration near the floor $C^*_{m,floor}$.

		Ceiling	Bottom	Side-up	Side-down
$\frac{C_{m,floor} \cdot Q}{S_{generator}}$	$d_p = 0.75\ \mu m$	0.23	0.74	0.94	0.64
	$d_p = 1.5\ \mu m$	0.23	0.73	0.93	0.63
	$d_p = 10\ \mu m$	0.18	0.43	0.62	0.42

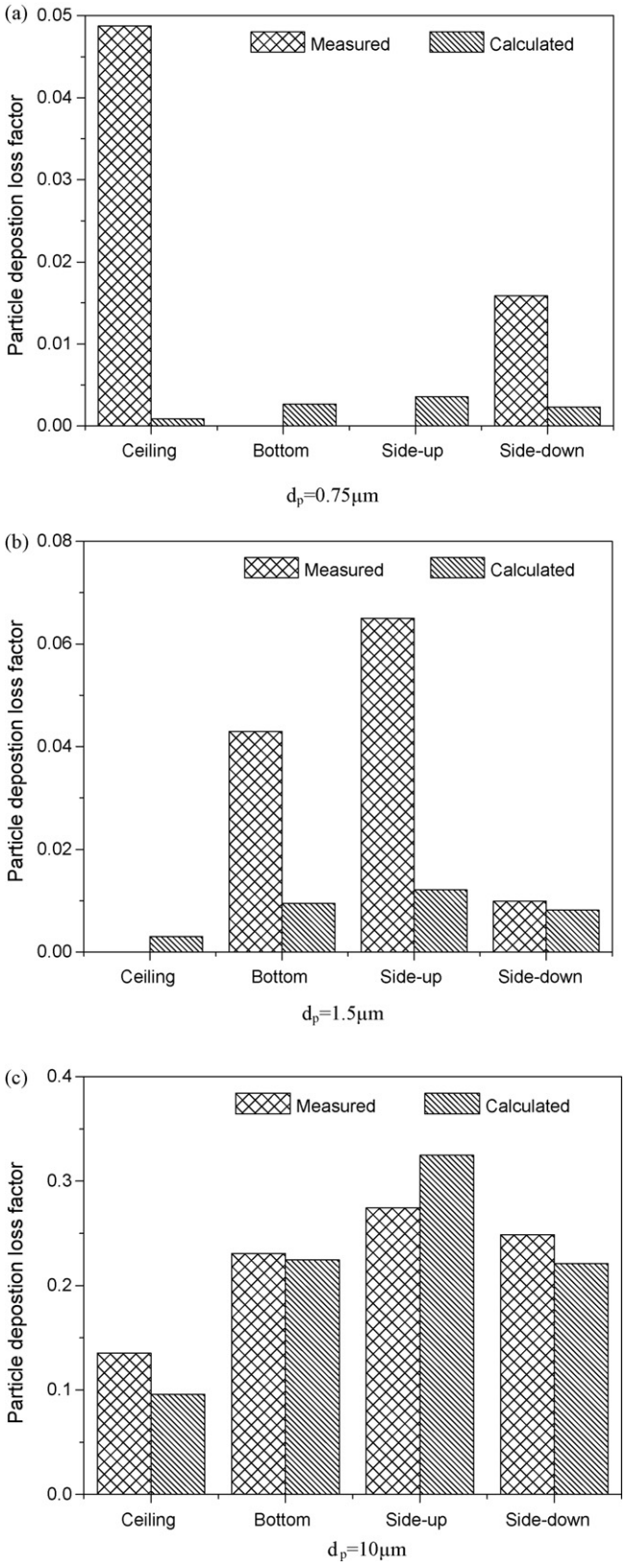

Fig. 3. Particle deposition loss factor of the four ventilation models.

influence of particle spatial distribution because the particle concentration at the outlet (C_{outlet}) is affected by both the airflow pattern and particle distribution. In other words, the difference in particle deposition on room surfaces attributed to varying particle spatial distribution is indirectly accounted for by the outlet particle concentration. This allows for differences in particle deposition under different ventilation modes to be incorporated into the model. We should also note that the total deposited particle quantity rate accounting for the particle spatial distribution, J (another expression for $S_{deposition}$), is:

$$J = \sum_{dA} J_{dA}$$
$$J_{dA} = V_{d-dA} C_{n-dA} dA, \quad (7)$$

where V_{d-dA} is the particle deposition velocity for the surface of each cell; C_{n-dA} is the particle concentration at grids adjacent to cell walls, dA is the wall area corresponding to each adjacent control volume, and J determines the outlet particle concentration according to mass balance principle. As C_{n-dA} reflects the particle distribution, thus the outlet concentration is determined by particle spatial distribution.

Both the measured and simulated deposited particle quantity under the four ventilation modes are displayed in Table 4 and Fig. 3, accounting for particle penetration and deposition loss factors (Eq. (5)). We can measure P/L as shown in Eqs. (1) and (5) by measuring particle generation rate and outlet concentration as mentioned before; they account for the particle spatial distribution as the outlet concentration is determined by particle distribution. We can also calculate these two values using the predicted particle concentration at the outlet (C_{out}) with assistance from a CFD simulation. This calculation is clarified in Section 2. Table 4 and Fig. 3 display the results from both the simulations and actual measurements.

As shown in Table 4 and Fig. 3, several of the optical particle counter measurements for smaller particles failed to yield concentrations above the limits of detection, resulting in relatively large error in the measured data and a discrepancy between the simulated and measured values. When particles are larger in diameter (d_p = 10 μm), however, the simulated results are in agreement with the measured data for all ventilation modes. When the particle diameter increased from 0.75 to 1.5 μm, the particle deposition loss factor increases just slightly. However, the particle deposition loss factor attains a larger increment rate when the particle diameter is 10 μm. For all sized particles, the deposition loss factor is largest using side-up supply ventilation. In contrast, we observed the smallest deposition loss factor under the ceiling supply mode and almost identical results for the other two ventilation modes.

As the particle deposition onto the floor plays the most important role and the result shown in Fig. 2 and Table 3 suggests the deposition velocity onto the floor varies little at different position on the floor, the mean concentration near the floor $C_{m,floor}$ (the concentration out of the particle concentration boundary layer, where the non-dimensional distance to the wall surfaces, y^+ is in the range of 200 according to [30]) becomes the largest determinant of the deposited particle quantity, implying that the particle spatial distribution as influenced by ventilation strategy plays a key role. This explains why, despite considerable difference in the particle deposition loss factor between the four ventilation modes, the mean deposition velocity/rate is almost identical across different modes. As shown in Table 5, the non-dimensional mean particle concen-

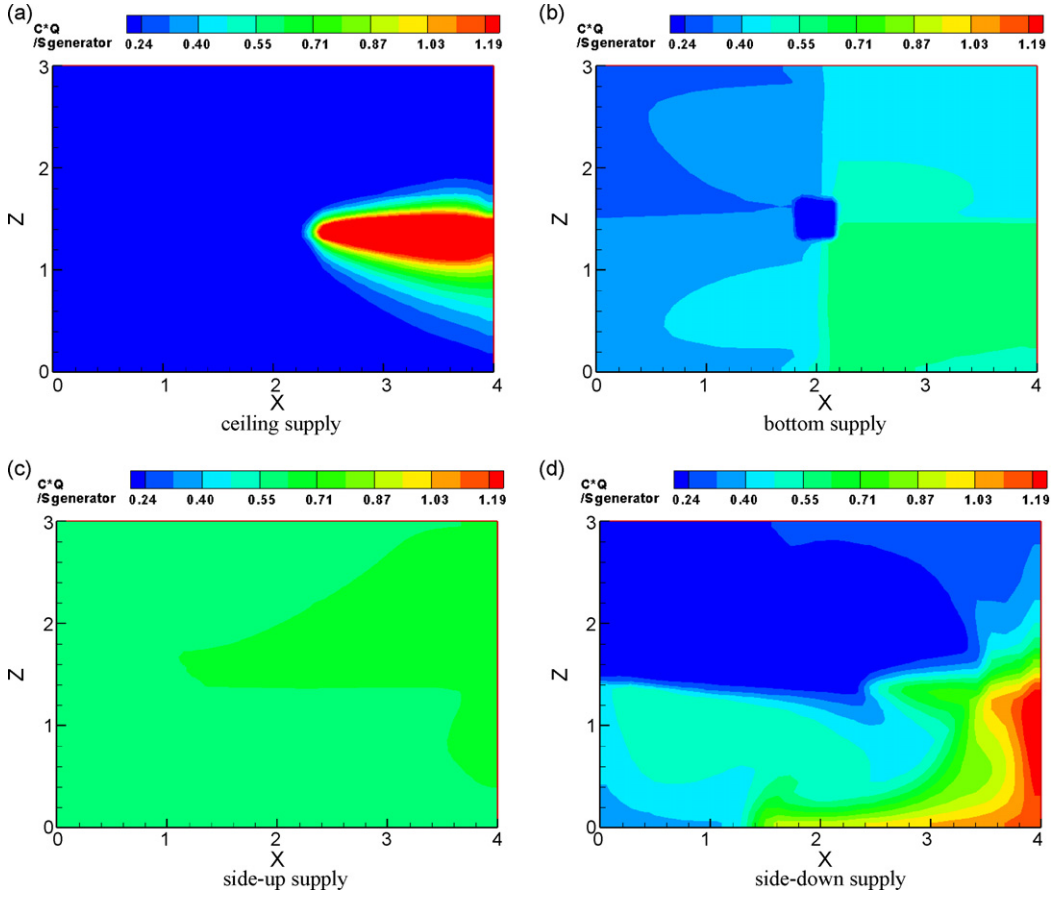

Fig. 4. The 10 μm particle concentration distribution near the floor (Y = 0.1 m).

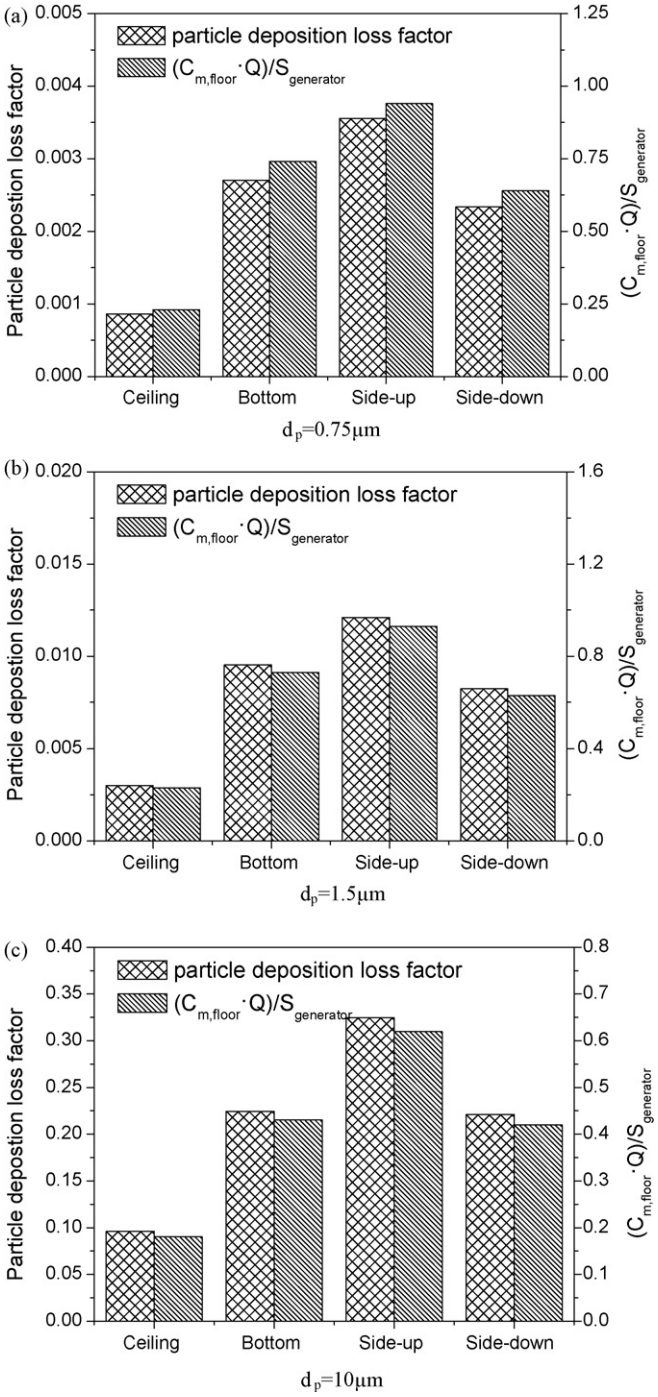

Fig. 5. Particle deposition loss factor and the mean particle concentration near the floor in four ventilation modes.

tration near the floor (defined as $C^*_{m,\mathrm{floor}} = (C_{m,\mathrm{floor}} \cdot Q)/S_{\mathrm{generator}}$) was largest during side-up supply ventilation, while that of ceiling supply is smallest and there are little differences between the other two ventilation strategies. Fig. 4 illustrates this finding using results from the 10 μm particle model. As shown in Fig. 5, the particle deposition loss factor almost in direct proportion to the non-dimensional mean concentration near the floor, when the particle size is in the range between 0.75 and 10 μm. This discrepancy between ventilation modes is attributable to the well mix of air and particles for the side-up supply mode, while the supply air of the side-down supply and the bottom supply cases push up the particles and thus leave a smaller concentration near the floor. In addition, the supply air from the ceiling inlet during the ceiling supply ventilation mode moves the particles directly up to the outlet on the vertical wall (X = 4.0 m). Consequently, there is minimal integration of air in the left half of the space (X < 2.0 m) with the air in the right half of the space (X > 2.0 m), leaving the smallest particle concentration near the floor. Due to the difference in particle spatial distribution, the particle deposition loss factor differs significantly between the four ventilation modes.

3.3. *Measures to control particle deposition/pollution in ventilated spaces*

Based on the above analysis, potential measures are suggested for controlling indoor particle pollution. When particle size falls within the studied range (0.75–10 μm), the ventilation modes and the location of the indoor particle source can have a significant influence on the indoor particle concentration and then the particle deposition.

Generally, when designing a ventilation mode, the airflow should move the particles directly up to the outlet, so the particle concentration in the breathing zone and near floor would be small. For this purpose, the possible location of the indoor particle source should be decided first and the outlet should be close to the particle source. The larger deposition particle quantity will lead to lower airborne particle concentration indoors, however, the deposited particle might resuspend into indoor air once there are enough energy, e.g., the disturbance of human activity or air flow. Thus the frequently cleaning of the surfaces is necessary to avoid particle pollution due to resuspension.

4. Discussion

We employed both numerical and experimental methods to investigate the deposition of different sized particles using four ventilation modes and a standard air supply volume (8 ACH). Unlike most exciting studies on this topic, the ventilation modes used in this are representative of those commonly used in both residential and commercial buildings. The results of our study can therefore be used to inform the development of building engineering projects that better control indoor microcontamination and, ultimately, benefit human health.

As mentioned above, the relative error of the deposition loss factor for fine particles (0.75–1.5 μm in diameter) is considerably larger than larger particles since the deposited particle quantity is very small (close to zero), and therefore beyond the measuring capacity of particle measurement instruments. Despite this limitation, however, our study indicates that use of different ventilation modes effects indoor particle deposition under operating conditions with the same particle-generating source and air supply volume. Future studies on this topic could benefit from use of additional experimental tests and particle monitoring equipment and more efforts may be deserved to contribute on finer particles that in nano range, which is not incorporated in present study.

The applicability of particle penetration factor P and particle deposition loss factor L is solely limited to a steady-state condition, i.e., the scenarios with continuous ventilation flow, a continuous source of particles and without disturbance of flow. The definition of penetrating factor P and deposition loss factor L are associated with indoor source strength. However, for the steady-state cases when the concentration at the inlet was zero, the particle concentration in any location of the ventilation room is linear to the particle source strength according to linear superposition theorem, which implies the penetrating factor P and deposition loss factor L was not related to the indoor source strength. The testification of this issue

by both theoretical and experimental approach can be found in a latest study [32].

5. Conclusion

Our study indicates the important influence of particle distribution on indoor particle deposition by both experimental and numerical methods. The following conclusions may be drawn based on our results:

(1) Though mean deposition velocity/rate for the studied particle sizes is not affected by the change of ventilation modes, the deposition loss factors differed considerably. Use of the mean deposition velocity/rate to estimate indoor particle deposition would therefore provide results that indicate a stable deposition quantity across different ventilation modes. However, the experiment and simulation tests conducted in our study demonstrate that ventilation does indeed affect particle deposition, indicating that mean deposition velocity/rate is not an appropriate metric for this purpose.
(2) Particle size and particle deposition are directly related, and deposition increases at an increasing rate, particularly above 10 μm.
(3) Gravitational settling plays the most important role on particle deposition when particle size falls into the range of 0.75–10 μm. The difference between the mean deposition velocity during the four ventilation modes is negligible (as shown in Fig. 2) and the concentration near the test room's floor becomes the main determinant of particle deposition quantity.
(4) When particle size falls within the 0.75–10 μm range, the ventilation strategy plays an important role in particle deposition by influencing the particle spatial distribution. The deposited particle quantity was largest near the floor during side-up supply ventilation, while that of ceiling supply is smallest and there are little differences between the other two ventilation strategies. We found that the particle loss factor during ventilation modes characterized by upward air flow through the room is smaller than that of mixing ventilation, however this trend was strongly influenced by the relative locations of the inlets, outlets and aerosol source.

Acknowledgements

This work was supported by grants from the National Key Technology Research and Development Program in China under contract 2006BAJ02A10 and the Fundamental Research Foundation at Tsinghua University under grant number Jcqn 2005002.

References

[1] W.W. Nazaroff, M.P. Ligocki, T. Ma, G.R. Cass, Particle deposition in museums: comparison of modeling and measurement results, Aerosol Science and Technology 13 (1990) 332–348.
[2] W.W. Nazaroff, G.R. Cass, Protecting museum collections from soiling due to the deposition of airborne particles, Atmospheric Environment 25A (1991) 841–852.
[3] M.A. Byrne, A.J.H. Goddard, C. Lange, J. Roed, Stable tracer aerosol deposition measurements in a test chamber, Journal of Aerosol Science 26 (1995) 645–653.
[4] L. Morawska, M. Jamriska, Deposition of radon progeny on indoor surfaces, Journal of Aerosol Science 27 (1995) 305–312.
[5] T.L. Thatcher, D.W. Layton, Deposition, resuspension and penetration of particles within a residence, Atmospheric Environment 29 (1995) 1485–1497.
[6] R. Aksu, H. Horvath, W. Kaller, S. Lahounik, P. Pesava, S. Toprak, Measurement of the deposition velocity of particulate matter to building surfaces in the atmosphere, Journal of Aerosol Science 27 (1996) s675–s676.
[7] C.L. Fogh, M.A. Byrne, J. Roed, A.J.H. Goddard, Size specific indoor aerosol deposition measurement and derived I/O concentrations ratios, Atmospheric Environment 31 (1997) 2193–2203.
[8] Y. Nomura, P.K. Hopke, B. Fitzgerald, B. Mesbah, Deposition of particles in a chamber as a function of ventilation rate, Aerosol Science and Technology 27 (1997) 62–72.
[9] M. Abadie, K. Limam, F. Allard, Indoor particle pollution: effect of wall textures on particle deposition, Building and Environment 36 (2001) 821–827.
[10] T.L. Thatcher, A.C.K. Lai, R. Moreno-Jackson, R.G. Sextro, W.W. Nazaroff, Effects of room furnishings and air speed on particle deposition rates indoors, Atmospheric Environment 36 (2002) 1811–1819.
[11] A.C.K. Lai, Particle deposition indoors: a review, Indoor Air 12 (2002) 211–214.
[12] C. Howard-Reed, L. Wallace, J. Emmerich, Effect of ventilation systems and air filters on decay rates of particles produced by indoor sources in an occupied townhouse, Atmospheric Environment 37 (2003) 5295–5306.
[13] C. He, L. Morawska, D. Gilbert, Particle deposition rates in residential houses, Atmospheric Environment 39 (2005) 3891–3899.
[14] W.W. Nazaroff, G.R. Cass, Mathematical modeling of indoor aerosol dynamics, Environmental Science and Technology 23 (1989) 157–165.
[15] M. Kulmala, A. Asmi, L. Pirjola, Indoor air aerosol model: the effect of outdoor air, filtration and ventilation on indoor concentrations, Atmospheric Environment 33 (1999) 2133–2144.
[16] T. Schneider, J. Kildeso, N.O. Breum, A two compartment model for determining the contribution of sources, surface deposition and resuspension to air and surface dust concentration levels in occupied rooms, Building and Environment 34 (1999) 583–595.
[17] C.Y.H. Chao, T.C. Tung, An empirical model for outdoor contaminant transmission into residential buildings and experimental verification, Atmospheric Environment 35 (2001) 1585–1596.
[18] B. Zhao, Y. Wang, B. Yan, PROBE-PM: A new way to simulate particle transport in ventilation systems, Building Simulation: An International Journal 1 (2008) 158–168.
[19] W. Lu, A.T. Howarth, Indoor aerosol particle deposition and distribution: numerical analysis for a one-zone ventilation system, Building Services Engineering Research and Technology 16 (1995) 141–147.
[20] W. Lu, A.T. Howarth, Numerical analysis of indoor aerosol particle deposition and distribution in two-zone ventilated system, Building and Environment 31 (1996) 41–50.
[21] B. Zhao, Y. Zhang, X. Li, X. Yang, D. Huang, Comparison of indoor aerosol particle concentration and deposition in different ventilated rooms by numerical method, Building and Environment 39 (2004) 1–8.
[22] B. Zhao, X. Li, Z. Zhang, Numerical study of particle deposition in two different kind of ventilated rooms, Indoor and Built Environment 13 (2004) 443–451.
[23] F. Chen, S.C.M. Yu, A.C.K. Lai, Modeling particle distribution and deposition in indoor environments with a new drift-flux model, Atmospheric Environment 40 (2006) 357–367.
[24] J. Bouilly, K. Limam, C. Beghein, F. Allard, Effect of ventilation strategies on particle decay rates indoors: an experimental and modeling study, Atmospheric Environment 39 (2005) 4885–4892.
[25] B. Zhao, J. Wu, Particle deposition in indoor environments: analysis of influencing factors, Journal of Hazardous Materials 147 (2007) 439–448.
[26] TSI Inc. Model 3475 Condensation Monodisperse Aerosol Generator Instruction Manual, 2004.
[27] Fluke Inc. Manual for Fluke 983 Optical Particle Counter, 2005.
[28] B. Zhao, X. Li, Q. Yan, A simplified system for indoor airflow simulation, Building and Environment 38 (2003) 543–555.
[29] Q. Chen, W. Xu, A zero-equation turbulence model for indoor air flow simulation, Energy and Buildings 28 (1998) 137–144.
[30] A.C.K. Lai, W.W. Nazaroff, Modeling indoor particle deposition from turbulent flow onto smooth surfaces, Journal of Aerosol Science 31 (2000) 463–476.
[31] B. Zhao, J. Wu, Particulate pollution in ventilated space: analysis of influencing factors, Journal of Hazardous Materials 163 (2009) 454–462.
[32] B. Zhao, J. Wu, Modeling particle fate in ventilation system—Part I: model development, Building and Environment 44 (2009) 605–611.